Cell Reports Medicine, Volume *5*

Supplemental information

Loss of p53 and SMAD4 induces adenosquamous subtype pancreatic cancer in the absence of an oncogenic KRAS mutation

Daowei Yang, Xinlei Sun, Rohan Moniruzzaman, Hua Wang, Citu Citu, Zhongming Zhao, Ignacio I. Wistuba, Huamin Wang, Anirban Maitra, and Yang Chen

Figure S1

A

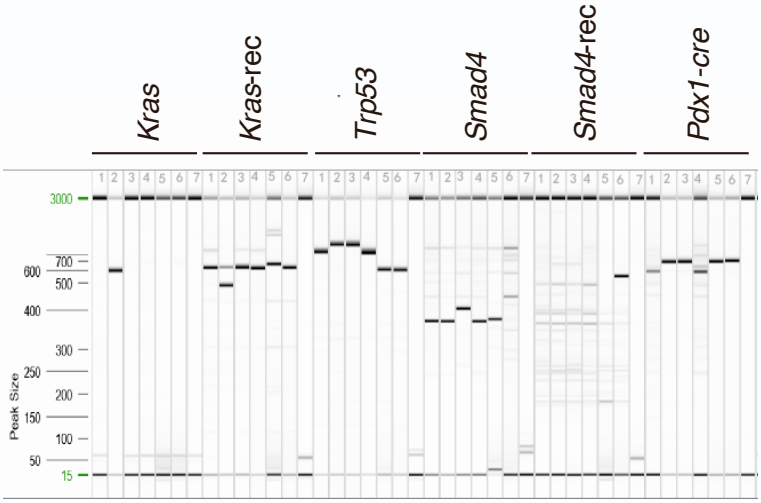

1	Tail-WT
2	Tail-KPPC
3	Tail-PPSSC
4	Pancreas-WT
5	Pancreas-KPPC
6	Pancreas-PPSSC
7	H_2O

B

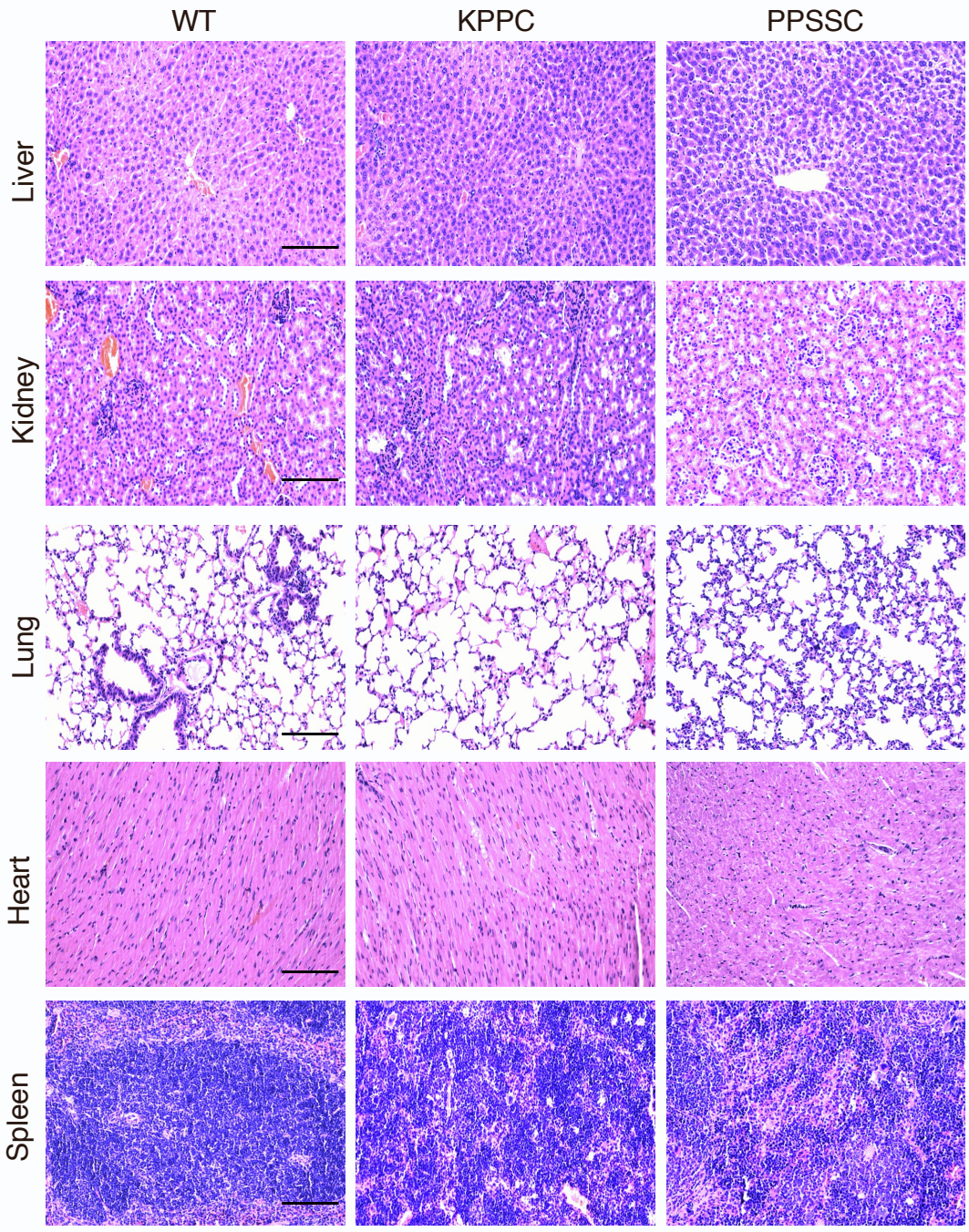

Figure S1. Characterization of the genotype and tissue histology for KPPC and PPSSC mice. Related to Figure 1.

(**A**) PCR product detection confirming the *Pdx1-Cre* specific deletion of *Smad4* and *Trp53*, as well as the presence of *LSL-Kras*^{G12D} and *Pdx1-Cre* in DNA samples from indicated mice. *Kras* recombination (*Kras*-rec) primers, *Smad4* recombination (*Smad4*-rec) primers, and *Trp53* flox primers were used to validate the *Pdx1-Cre*-mediated recombination of *LSL-Kras*^{G12D}, *Smad4*$^{loxP/loxP}$, and *Trp53*$^{loxP/loxP}$ alleles, respectively.

(**B**) Comparison of the histology by H&E staining on a variety of tissues from KPPC mice (2.5-month-old) and PPSSC mice (8-month-old), as compared with tissues from normal (WT) mice (2.5-month-old). Scale bar: 100 μm.

Figure S2

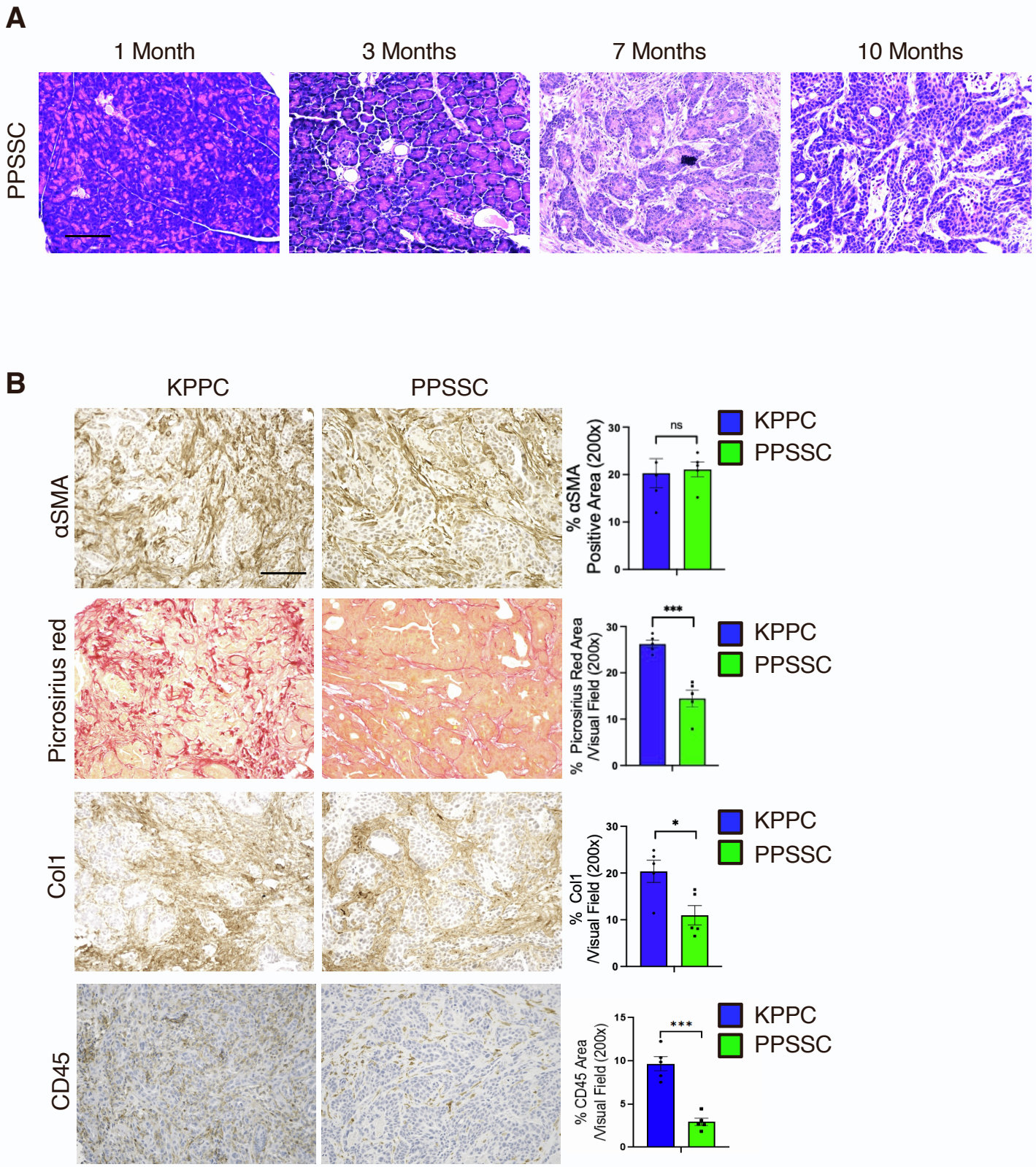
A
1 Month
3 Months
7 Months
10 Months
PPSSC
B
KPPC
PPSSC
αSMA
% αSMA Positive Area (200x)
ns
KPPC
PPSSC
Picrosirius red
% Picrosirius Red Area /Visual Field (200x)
***
KPPC
PPSSC
Col1
% Col1 /Visual Field (200x)
*
KPPC
PPSSC
CD45
% CD45 Area /Visual Field (200x)
***
KPPC
PPSSC

Figure S2. Additional characterization of the tumor histology for PPSSC and KPPC tumors. Related to Figure 1.

(**A**) Pancreatic tissue histology of PPSSC mice at various ages from 1 month to 10 months. Scale bar: 100 μm.

(**B**) Representative images of immunohistochemistry staining for alpha-smooth muscle actin (αSMA), type I collagen (Col1), and CD45 on pancreatic tumor sections from KPPC mice (2.5-month-old) and stage-matched PPSSC mice (8-month-old). Picrosirius red staining was used for collagen fibers visualization. Quantitative results were shown with Student's *t* test. Scale bar: 100 μm. * $P < 0.05$, *** $P < 0.001$. ns: not significant.

Figure S3

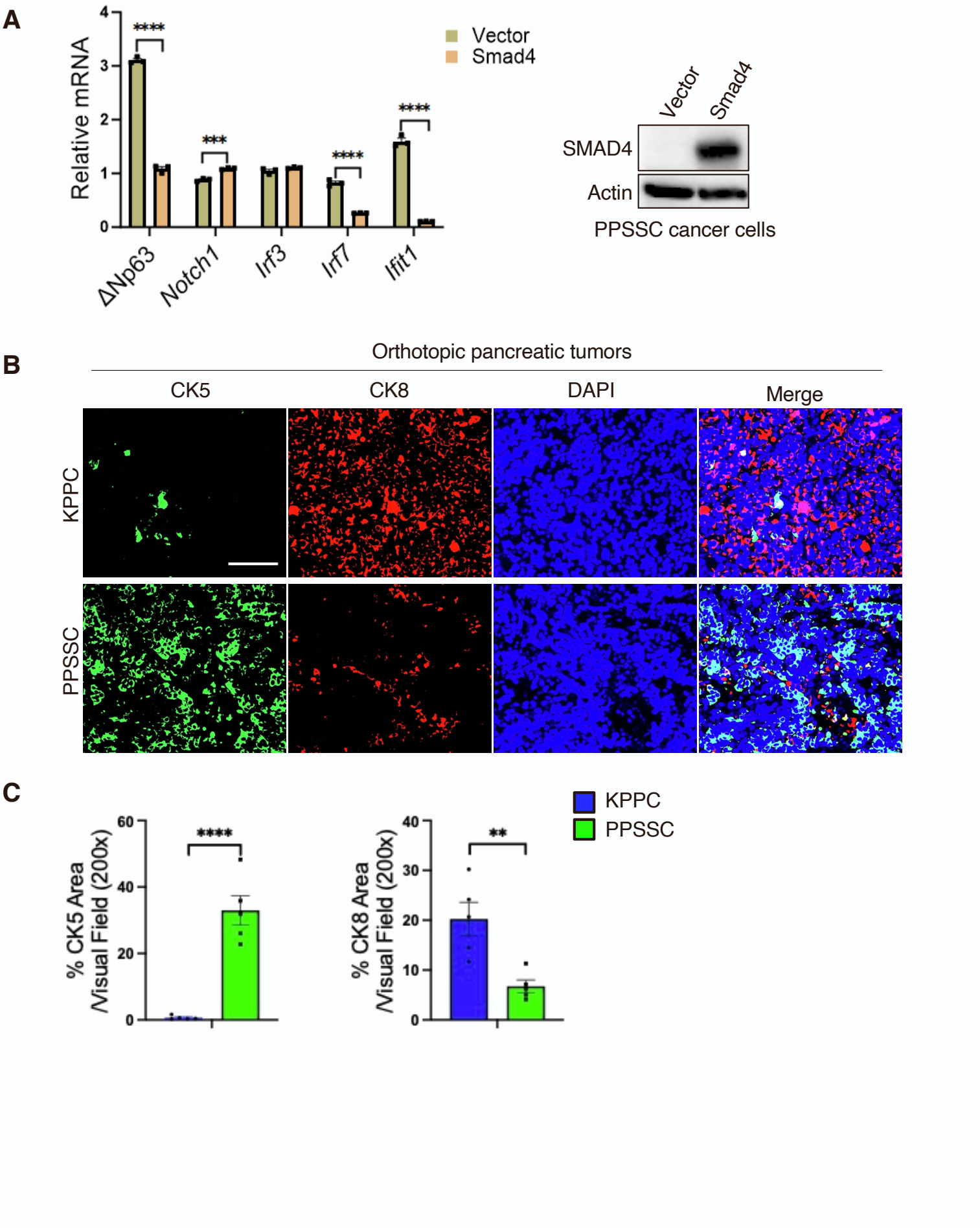
A
Relative mRNA
Vector
Smad4
****
***
****
****
ΔNp63
Notch1
Irf3
Irf7
Ifit1
Vector
Smad4
SMAD4
Actin
PPSSC cancer cells
B
Orthotopic pancreatic tumors
CK5
CK8
DAPI
Merge
KPPC
PPSSC
C
KPPC
PPSSC
% CK5 Area /Visual Field (200x)
****
% CK8 Area /Visual Field (200x)
**

Figure S3. Expression profile of cytokeratin (CK) markers in orthotopic pancreatic tumors formed by KPPC and PPSSC cancer cell lines. Related to Figure 3.

(**A**) qRT-PCR analysis of ΔNp63, *Notch1*, *Irf3*, *Irf7*, and *Ifit1* expression levels in PPSSC cancer cells transfected with either a vector of SMAD4 expression or a control vector (n = 3 biological replicates). Western blot assay validated the SMAD4 expression in PPSSC cancer cells transfected with SMAD4-expressing vector. Gene expression levels were compared with Student's *t* test. *** $P < 0.001$, **** $P < 0.0001$.

(B) Representative images of immunofluorescence staining for CK5 (green), CK8 (red), and nuclei/DAPI (blue) in orthotopic pancreatic tumors (n = 5 per group) formed by KPPC and PPSSC cancer cell lines. Scale bar: 100 μm.

(**C**) Quantitative analysis of CK5 and CK8 positive staining shown in (**B**). Results were shown with Student's *t* test. ** $P < 0.01$, **** $P < 0.0001$.

Figure S4

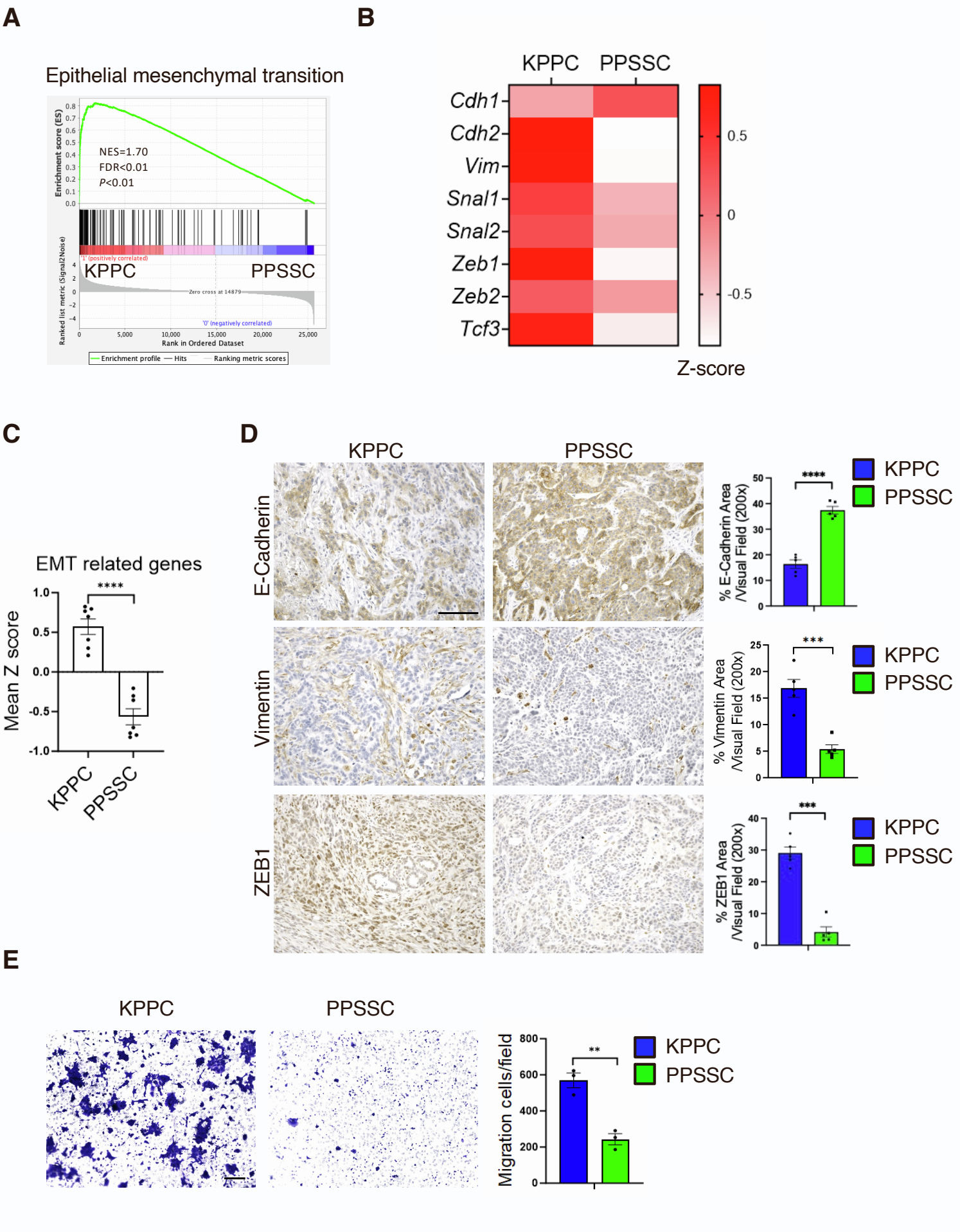
A
Epithelial mesenchymal transition
NES=1.70
FDR<0.01
P<0.01
KPPC
PPSSC
Enrichment score (ES)
Ranked list metric (Signal2Noise)
Rank in Ordered Dataset
Enrichment profile
Hits
Ranking metric scores
B
KPPC
PPSSC
Cdh1
Cdh2
Vim
Snal1
Snal2
Zeb1
Zeb2
Tcf3
0.5
0
-0.5
Z-score
C
EMT related genes
Mean Z score
****
KPPC
PPSSC
D
KPPC
PPSSC
E-Cadherin
Vimentin
ZEB1
% E-Cadherin Area /Visual Field (200x)
% Vimentin Area /Visual Field (200x)
% ZEB1 Area /Visual Field (200x)
****
***
***
KPPC
PPSSC
E
KPPC
PPSSC
Migration cells/field
**
KPPC
PPSSC

Figure S4. Characterization of epithelial-to-mesenchymal transition (EMT) phenotype in KPPC and PPSSC cancer cell lines. Related to Figure 3.

(**A**) Gene Set Enrichment Analysis (GSEA) of RNA-seq data on KPPC and PPSSC cancer cell lines. EMT-associated genes were downregulated in PPSSC cancer cells, as compared with KPPC cancer cells.

(**B and C**) Heatmap showing the gene expression levels of EMT-related genes between KPPC and PPSSC cancer cell lines (**B**). The mean Z-score of these genes was compared with Student's *t* test (**C**). **** $P < 0.0001$.

(**D**) Representative images of immunohistochemistry staining for E-Cadherin, Vimentin, and ZEB1 on pancreatic tumor sections from KPPC mice (2.5-month-old) and stage-matched PPSSC mice (8-month-old). Quantitative results were also shown with Student's *t* test. Scale bar: 100 μm. *** $P < 0.001$, **** $P < 0.0001$.

(**E**) Representative images of transwell migration assay on KPPC and PPSSC cancer cell lines (n = 3 biological replicates). The migrated cells attached to the bottom layer of transwell membrane were counted. Results were shown with Student's *t* test. ** $P < 0.01$.

Figure S5

A

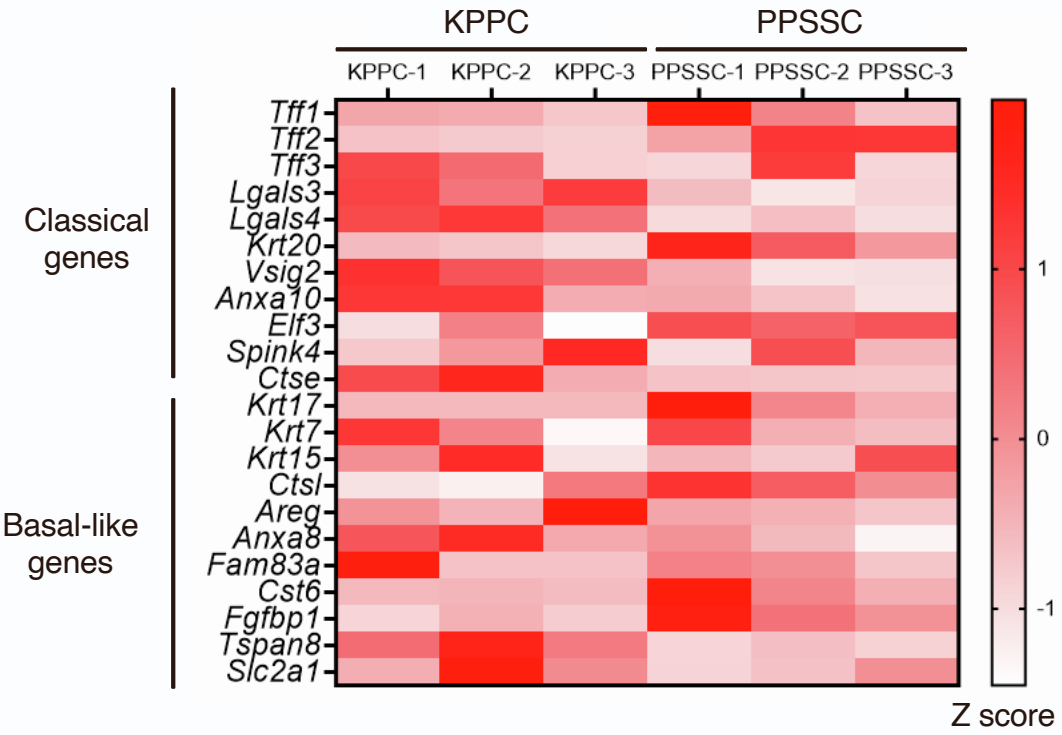
KPPC
PPSSC
KPPC-1
KPPC-2
KPPC-3
PPSSC-1
PPSSC-2
PPSSC-3
Classical genes
Basal-like genes
Tff1
Tff2
Tff3
Lgals3
Lgals4
Krt20
Vsig2
Anxa10
Elf3
Spink4
Ctse
Krt17
Krt7
Krt15
Ctsl
Areg
Anxa8
Fam83a
Cst6
Fgfbp1
Tspan8
Slc2a1
1
0
-1
Z score

B

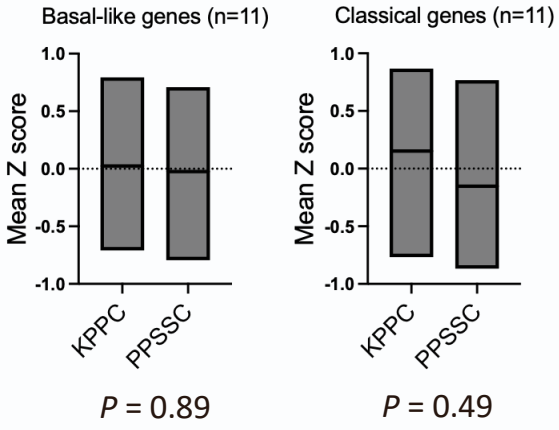
Basal-like genes (n=11)
Classical genes (n=11)
Mean Z score
1.0
0.5
0.0
-0.5
-1.0
KPPC
PPSSC
P = 0.89
P = 0.49

Figure S5. The expression levels of basal-like and classical subtype genes in KPPC and PPSSC cancer cells. Related to Figure 3.

(**A**) Heatmap showing the expression profiles of basal-like and classical subtype genes in KPPC and PPSSC cancer cells.

(**B**) Box plots comparing the mean Z-scores of basal-like and classical subtype genes shown in **A**.

Figure S6

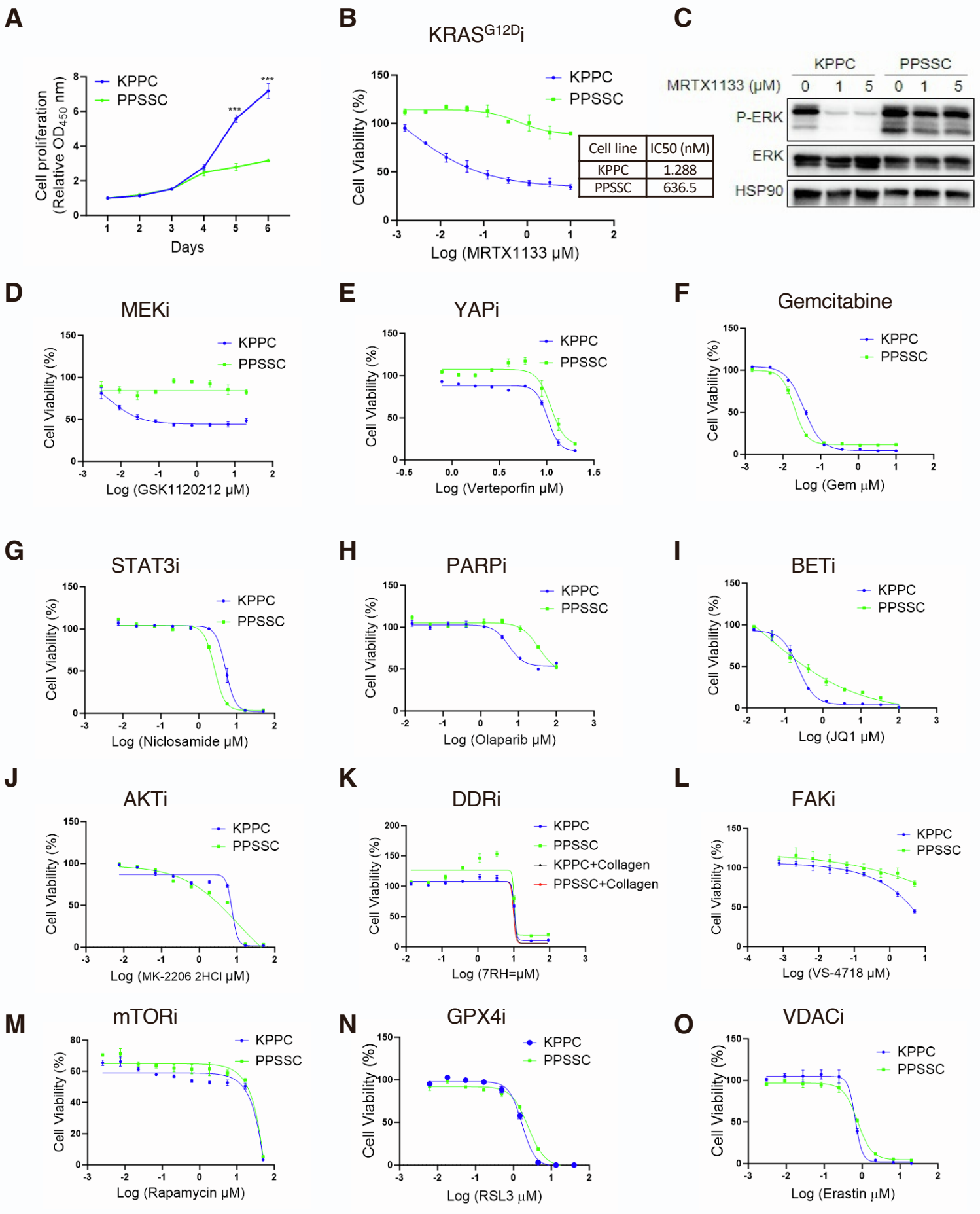
A
Cell proliferation (Relative OD450 nm)
KPPC
PPSSC
***
***
Days
B
KRASG12Di
Cell Viability (%)
KPPC
PPSSC
Cell line | IC50 (nM)
KPPC | 1.288
PPSSC | 636.5
Log (MRTX1133 μM)
C
KPPC
PPSSC
MRTX1133 (μM) 0 1 5 0 1 5
P-ERK
ERK
HSP90
D
MEKi
Log (GSK1120212 μM)
E
YAPi
Log (Verteporfin μM)
F
Gemcitabine
Log (Gem μM)
G
STAT3i
Log (Niclosamide μM)
H
PARPi
Log (Olaparib μM)
I
BETi
Log (JQ1 μM)
J
AKTi
Log (MK-2206 2HCl μM)
K
DDRi
KPPC+Collagen
PPSSC+Collagen
Log (7RH=μM)
L
FAKi
Log (VS-4718 μM)
M
mTORi
Log (Rapamycin μM)
N
GPX4i
Log (RSL3 μM)
O
VDACi
Log (Erastin μM)

Figure S6. Characterization of primary cancer cell lines from KPPC and PPSSC tumors. Related to Figure 3.

(**A**) Cell proliferation of KPPC and PPSSC cancer cell lines over time (n = 3 biological replicates). One-way ANOVA with Tukey's multiple comparison test was used to compare these two groups. *** $P < 0.001$.

(**B**) Cell viability of KPPC and PPSSC cancer cell lines (% normalized to the untreated group of each cell line) treated with MRTX1133 (n = 3 biological replicates). IC50 values of MRTX1133 in PPSSC and KPPC cancer cells were also shown.

(**C**) Detection of phospho-ERK (P-ERK) and total ERK in KPPC and PPSSC cancer cell lines treated with MRTX1133 at indicated concentrations for three hours by Western blot assay.

(**D-O**) Cell viability of KPPC and PPSSC cancer cell lines (% normalized to untreated group of each cell line) treated with MEK inhibitor GSK1120212 (**D**), YAP inhibitor Verteporfin (**E**), Gemcitabine (Gem) (**F**), STAT3 inhibitor Niclosamide (**G**), PARP inhibitor Olaparib (**H**), BET inhibitor JQ1 (**I**), AKT inhibitor MK-2206 (J), DDR1 inhibitor 7RH (with or without type I collagen coating) (**K**), FAK inhibitor VS-4718 (**L**), mTOR inhibitor Rapamycin (**M**), GPX4 inhibitor RSL3 (**N**), and VDAC inhibitor Erastin (**O**) (n = 3 biological replicates).

Figure S7

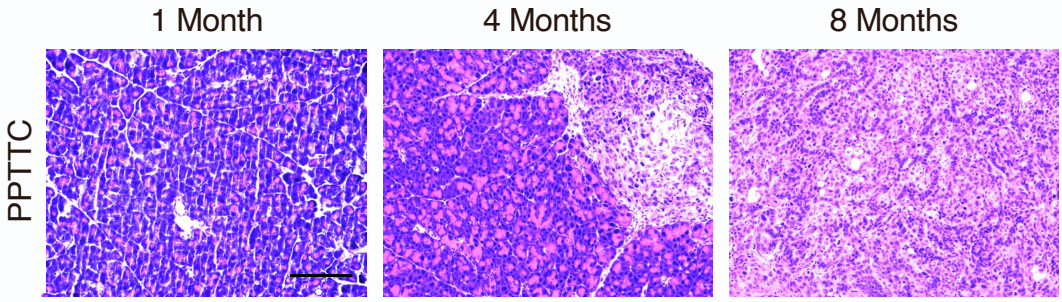

Figure S7. Pancreatic tissue histology of PPTTC mice at various ages. Related to Figure 4.

Comparison of pancreatic tissue histology by H&E staining of PPTTC mice at various ages from 1 month to 8 months. Scale bar: 100 μm.

Figure S8

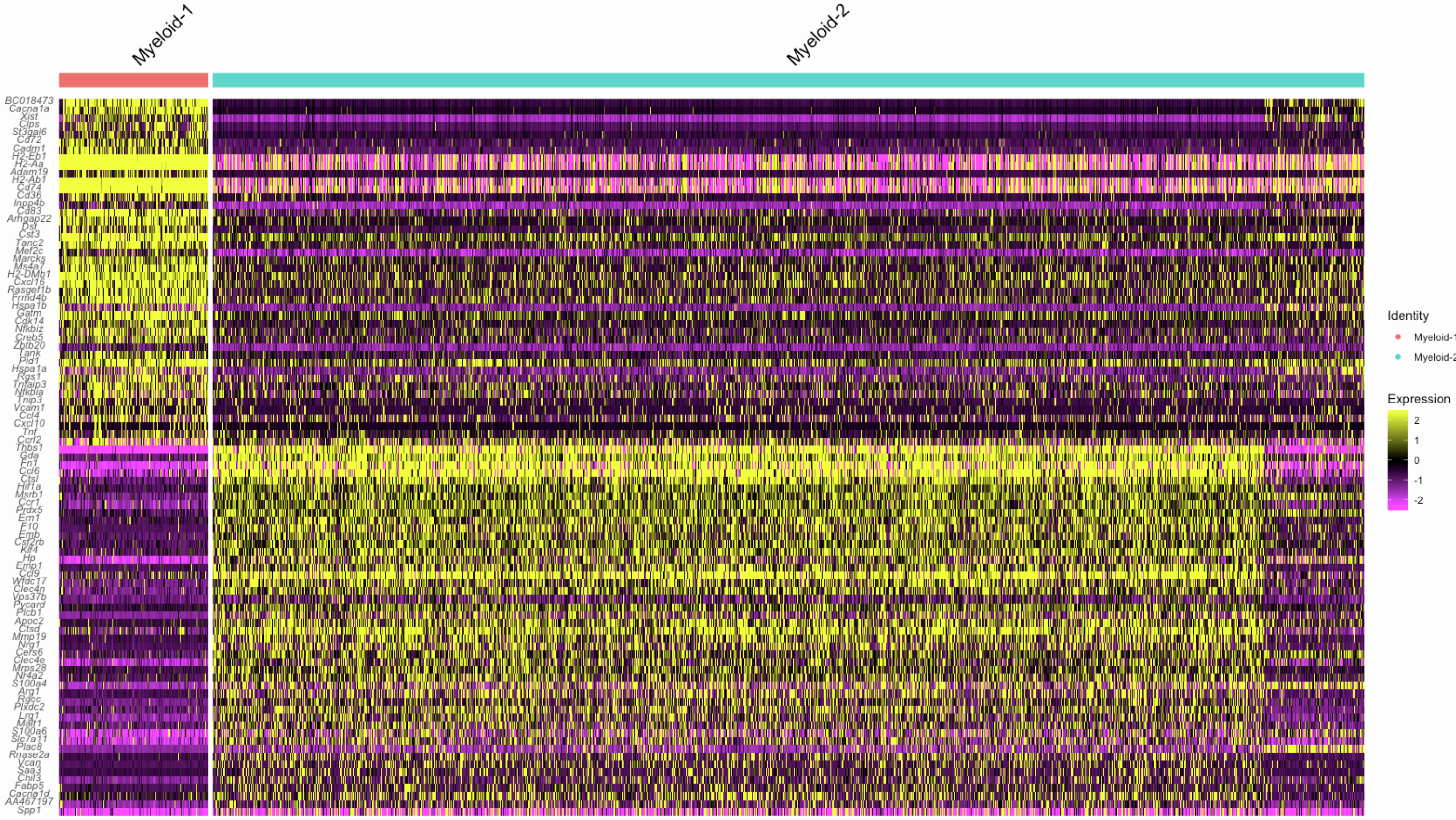
Myeloid-1
Myeloid-2
Identity
Myeloid-1
Myeloid-2
Expression
2
1
0
-1
-2

Figure S8. Single-cell analysis showing the expression profiles of signature genes of Myeloid-1 and Myeloid-2 cell subclusters. Related to Figure 5.

Expression profiles of signature genes shown in heatmap for Myeloid-1 and Myeloid-2 in KPPC and PPSSC tumors.

Figure S9

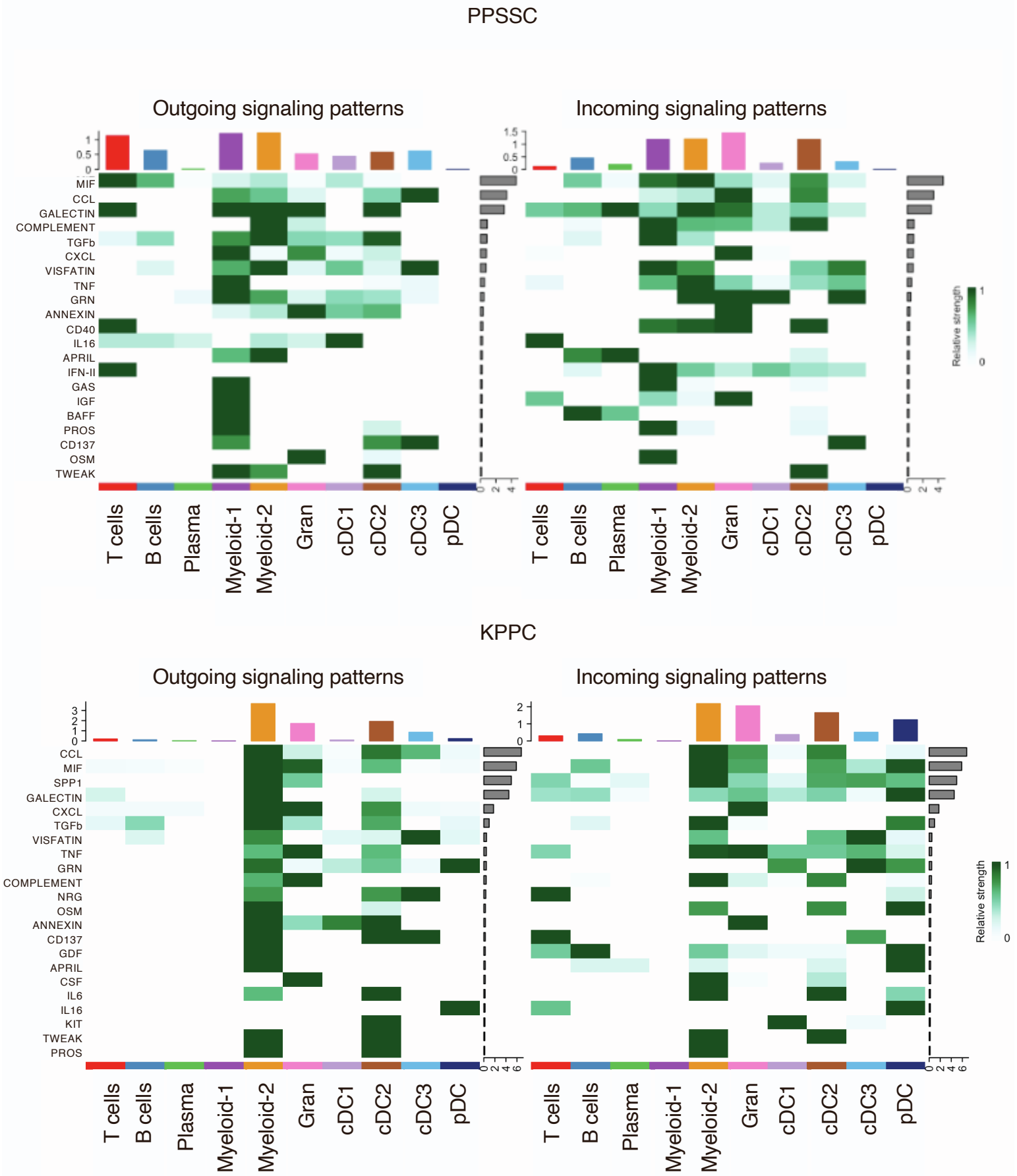
PPSSC
Outgoing signaling patterns
Incoming signaling patterns
MIF
CCL
GALECTIN
COMPLEMENT
TGFb
CXCL
VISFATIN
TNF
GRN
ANNEXIN
CD40
IL16
APRIL
IFN-II
GAS
IGF
BAFF
PROS
CD137
OSM
TWEAK
T cells
B cells
Plasma
Myeloid-1
Myeloid-2
Gran
cDC1
cDC2
cDC3
pDC
Relative strength
KPPC
Outgoing signaling patterns
Incoming signaling patterns
CCL
MIF
SPP1
GALECTIN
CXCL
TGFb
VISFATIN
TNF
GRN
COMPLEMENT
NRG
OSM
ANNEXIN
CD137
GDF
APRIL
CSF
IL6
IL16
KIT
TWEAK
PROS
T cells
B cells
Plasma
Myeloid-1
Myeloid-2
Gran
cDC1
cDC2
cDC3
pDC
Relative strength

Figure S9. The signaling pathways of cell-cell communication networks across various immune cells in KPPC and PPSSC tumors. Related to Figure 5.

The cell-cell communication intensity of indicated signaling pathways across various immune cell populations in PPSSC and KPPC tumors. The outgoing signaling and incoming signaling patterns were separately shown in the heatmap.

Figure S10

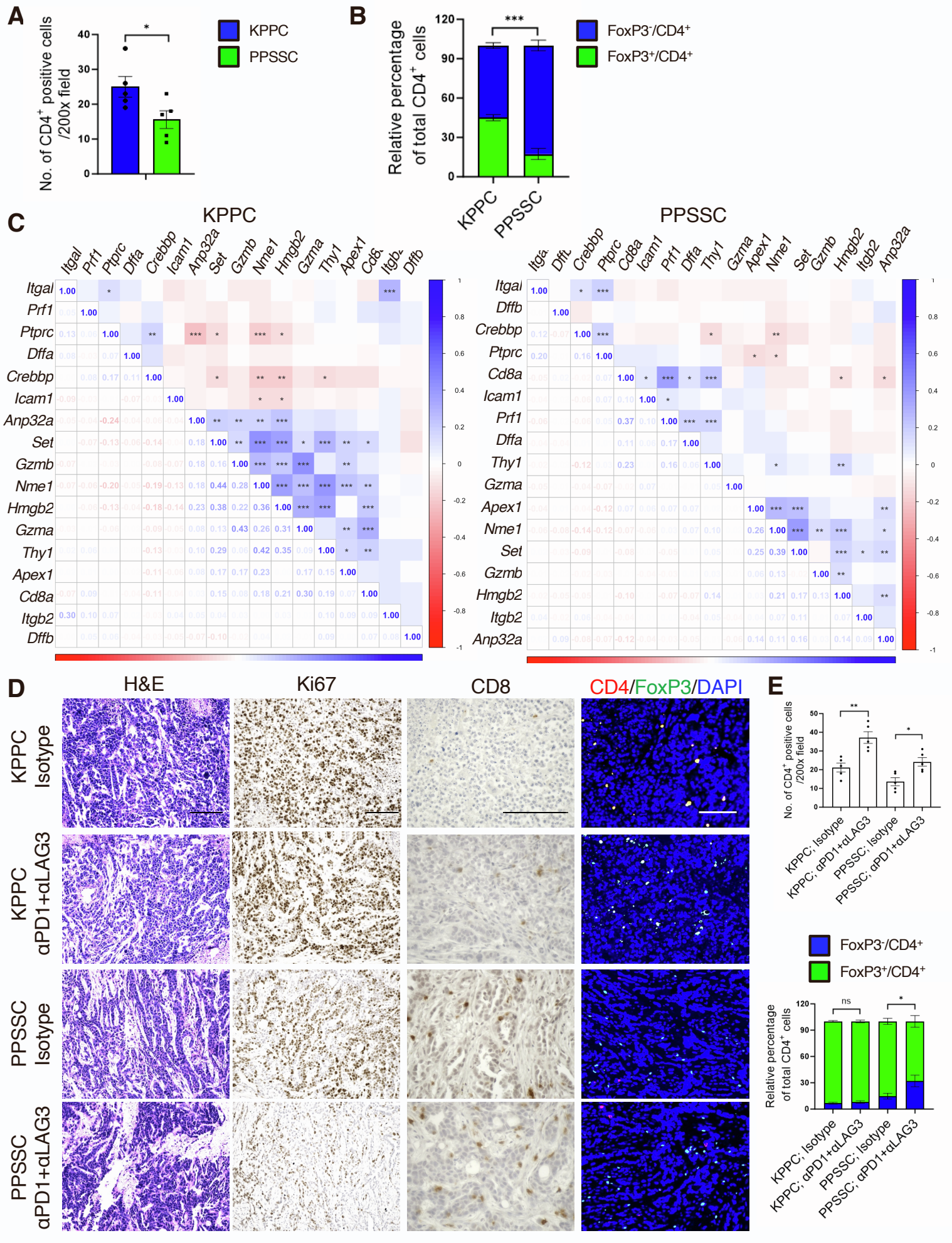
A
No. of CD4+ positive cells /200x field
KPPC
PPSSC
B
Relative percentage of total CD4+ cells
FoxP3-/CD4+
FoxP3+/CD4+
C
KPPC
PPSSC
D
H&E
Ki67
CD8
CD4/FoxP3/DAPI
KPPC Isotype
KPPC αPD1+αLAG3
PPSSC Isotype
PPSSC αPD1+αLAG3
E
KPPC; Isotype
KPPC; αPD1+αLAG3
PPSSC; Isotype
PPSSC; αPD1+αLAG3
ns

Figure S10. Characterization of T cells in KPPC and PPSSC tumors. Related to Figure 7.

(**A and B**) Quantitative analysis of immunofluorescence staining images described in **Figure 7F**. The numbers of total $CD4^+$ T cells (**A**), $FoxP3^+/CD4^+$ T cells (**B**), and $FoxP3^-/CD4^+$ T cells (**B**) were quantified respectively. Results were shown with Student's *t* test. * $P < 0.05$, *** $P < 0.001$.

(**C**) The correlation analysis of *Cd8a* and cytotoxic T cell-related genes in $CD8^+$ T cells. Correlation strength was shown in the heatmap.

(**D and E**) Representative images of H&E staining, Ki67 staining, CD8 staining, and CD4/FoxP3/DAPI immunofluorescence staining on orthotopic pancreatic tumors with indicated treatments. The numbers of total $CD4^+$ T cells, $FoxP3^+/CD4^+$ T cells, and $FoxP3^-/CD4^+$ T cells were quantified respectively and were shown in **E.** Scale bar: 100 μm. * $P < 0.05$, ** $P < 0.01$.